ＩＳＳＮ１３４６−７８３２

独立行政法人港湾空港技術研究所

港湾空港技術研究所報告

REPORT OF THE PORT AND AIRPORT RESEARCH INSTITUTE

VOL.40　NO.3　September 2001

NAGASE, YOKOSUKA, JAPAN

INDEPENDENT ADMINISTRATIVE INSTITUTION,
PORT AND AIRPORT RESEARCH INSTITUTE

港湾空港技術研究所報告 (REPORT OF PARI)

第 40 巻 第 3 号 (Vol.40, No.3), 2001 年 9 月 (September 2001)

目　　次 (CONTENTS)

港湾空港技術研究所報告
第40巻第3号（2001.9）

せん断補強のない高性能軽量コンクリートはりのせん断耐荷機構

横田　弘*・舟橋　政司**・山田　昌郎***・原　夏生**・二羽　淳一郎****

要　旨

従来の人工軽量骨材の欠点であった強度および耐久性の問題を克服した高性能人工軽量骨材が近年開発された．この骨材を用いることで，海洋環境下においても所要の性能を満たす軽量コンクリート構造物を建造することが可能で，顕著な建設コスト縮減効果を期待できる場合があることを既に報告した．

その際，高性能軽量コンクリート部材のせん断耐力は，通常の砕石コンクリートのそれに比べて低下することが確認された．球形の人工軽量骨材を用いたコンクリートは，骨材の形状に起因する欠点として，コンクリートのせん断強度が低下する傾向を示す．そのため，土木学会コンクリート標準示方書では，従来の軽量コンクリートはりに対して，コンクリートの分担するせん断力を普通コンクリートのそれの70%に一律に低減させて対応している．これは，従来の人工軽量骨材コンクリートより得られた結果をベースとしているので，この低減係数の高性能人工軽量骨材コンクリートへの適用性を精査する必要がある．

このようなことから，せん断補強を有しない高性能軽量コンクリートはりのせん断載荷試験を行い，実験的にこの課題について考察した．その結果，高性能軽量コンクリートはりのせん断耐力は，コンクリートの単位容積質量が小さくなるにつれて低下することが確認された．そこで，せん断耐力の算定において，斜めひび割れ発生耐力をコンクリートの単位容積質量の関数とする低減係数を提案した．また，せん断スパン比に応じてせん断抵抗機構が変化し，通常コンクリートの破壊形態の性状が異なることが明らかとなった．

キーワード：高性能軽量コンクリート，人工軽量骨材，はり，せん断耐力，単位容積質量，低減係数

---

* 地盤・構造部　構造強度研究室長
** 前田建設工業株式会社　技術研究所
*** 前港湾技術研究所　構造部主任研究官（現・国土交通省下関港湾空港技術調査事務所副所長）
**** 東京工業大学大学院教授　理工学研究科土木工学専攻
239-0826　横須賀市長瀬3丁目1番1号　独立行政法人港湾空港技術研究所
Tel: 0468-44-5059, Fax: 0468-44-0255, Email: hiroy@cc.phri.go.jp

REPORT OF THE PORT AND
AIRPORT RESEARCH INSTITUTE
Vol.40, No.3 (Sept. 2001)

Shear Resisting Behavior of Super Lightweight Concrete Beams Without Web Reinforcement

Hiroshi YOKOTA*
Masashi FUNAHASHI**
Masao YAMADA***
Natsuo HARA**
Junichiro NIWA ****

Synopsis

The artificial super lightweight aggregate (SLA) with isolated void has recently been developed in Japan, which is characterized as the water absorption of about 3% and a density ranged from 850 to 1200kg/m^3. Concrete mixed with SLA exhibits excellent performances compared to that with conventional lightweight aggregates. Therefore, SLA concrete has high potential for use in various infrastructures including marine structures.

It is well known that the low crushing load and the spherical shape of artificial lightweight aggregates may cause deficiencies in load carrying capacities against shear or tensile forces. For example in the current JSCE standard specification, the shear capacity of a lightweight concrete beam is reduced to be 70% as that of general normal-weight concrete. This value for reduction was based on experimental studies on conventional lightweight aggregate concrete beams. Therefore, the applicability of this reduction to SLA concrete beams has to be confirmed.

Reinforced SLA concrete beams with the controlled density of concrete were experimentally load-tested. The test results showed that the shear capacity becomes low as the density of concrete is decreased. The conversion term from general normal-weight concrete to SLA concrete for calculating the ultimate shear strength was proposed based on the test results, which is a function of the density of concrete. The shear resisting mechanism of SLA concrete beams was discussed with the shear span to effective depth ratio.

Key Words: super lightweight concrete, beam, shear resistance, density, conversion term

* Head, Structural Mechanics Division, Geotechnical and Structural Engineering Department
** Technical Research Institute, Technology Division, Maeda Corporation
*** Ex-Senior Research Engineer, Structural Engineering Division, Port and Harbour Research Institute
**** Professor, Department of Civil Engineering, Tokyo Institute of Technology
3-1-1, Nagase, Yokosuka, 239-0826
Phone: +81-468-445059, Fax: +81-468-440255, E-mail: hiroy@cc.phri.go.jp

CONTENTS

1. Introduction

As external forces become increase because of enlargement of ship sizes or severe natural conditions in deep-sea areas, marine structures particularly those constructed in ports have become larger nowadays, and it is likely that this trend will continue. A reinforced concrete caisson, widely used as a principal structure of breakwaters and quay walls, is a typical gravity type structure to resist external forces by its own weight. Therefore, a caisson has been regarded that its heavy weight is important requirement. On the other hand, the enlargement of structures requires, for an example, a large floating dock on which a caisson is built. Moreover, construction methods may become rather complicated in marine areas because of draft restrictions imposed for towing of the caisson.

Use of lightweight concrete to build the caisson is of great advantage in this regard as it releases some of the restrictions imposed by the construction method on the weight, size, and shape of which completed. The authors (Yokota et al., 2000a) compared two caissons for quay walls made of general normal-weight concrete and lightweight concrete. Use of lightweight concrete decreases the draft of the caisson; consequently, the structure can be made much slender in case that execution conditions such as draft restrictions or dock capacities are critical for dimensioning the caisson. This may result in significant reduction in construction cost and period.

There are several methods to achieve lightweight concrete. One of them is replacing fine or coarse aggregate in concrete with lightweight ones. Artificial super lightweight aggregate (abbreviated as SLA in this paper) with isolated void has recently been invented in Japan. SLA is characterized as the water absorption of about 3% and a density ranged from 850 to 1200kg/m^3, which is extremely superior to conventional artificial lightweight aggregate made of expanded shale. Concrete mixed with SLA exhibits excellent mechanical performances and durability compared to concrete mixed with conventional lightweight aggregate (Okamoto et al., 1999). The applicability of SLA concrete to marine structures was discussed in the authors' previous paper (Yokota et al., 2000b) from the viewpoints of durability and basic mechanical properties and it was concluded that SLA concrete has great potential for use there particularly for caissons.

It is well known, however, that the low crushing load and the spherical shape of artificial lightweight aggregate may cause deficiencies in load carrying capacities against shear or tensile forces. For example in the current JSCE standard specification for concrete structures (1996), the shear capacity of a lightweight concrete beam is constantly reduced to be 70% as that of general normal-weight concrete. This value for reduction is based on experimental studies on conventional lightweight aggregate concrete beams. Therefore, the validity of this reduction to SLA concrete beams has to be confirmed.

Reinforced SLA concrete beams with controlled density of concrete were experimentally load-tested to discuss their shear resisting capacities. The test results showed that the shear capacity becomes low as the density of concrete is decreased. The conversion term from general normal-weight concrete to SLA concrete for calculating the ultimate shear strength was proposed based on the test results, which is a function of the density of concrete. It was also made clear that the shear resisting mechanism of SLA concrete beams depends on the shear span to effective depth ratio.

2. Artificial Super Lightweight Aggregate

Attempts to reduce the weight of concrete have been undertaken to date, but the application of conventional lightweight concrete has been limited because of many problems, such as the relatively small amount of weight reduction that can be achieved and poor durability and workability. Conventional artificial lightweight aggregate made of expanded shale is highly absorptive (the water absorption of 10% or more) owing to interconnected internal pores. In addition, expanded shale aggregate concrete is not very durable because of its low freeze-thaw resistance and is difficult to work with because of poor workability during pumping. These deficiencies have made Japanese engineers hesitate to use conventional lightweight aggregate concrete in civil engineering structures.

SLA, however, can overcome these drawbacks by successfully producing isolated void. Some comparisons between conventional lightweight aggregate and SLA are presented in **Table 1**. The crushing load of one SLA particle of 14mm in diameter is more than 800N and the water absorption is considerably low, about 3 to 5%. By mixing SLA with an appropriate amount of natural aggregate in concrete, it is now possible to obtain super lightweight concrete whose density ranges from approximately 1200 to 1800kg/m^3, while that of conventional lightweight concrete is about 2000kg/m^3. This reduction in the weight of concrete itself will be of great advantage for use as a construction material in civil engineering structures.

There are two kinds of SLA as listed in **Table 1**: the specified density of 850kg/m^3 and 1200kg/m^3. Because the sizes of the two aggregate are identical, the heavier one has larger crushing load and lower water absorption, that is, superior performance to the lighter one; but costs

Table 1 Fundamental specific properties of artificial lightweight aggregate

	Conventional	Recently invented SLA	
Density (kg/m^3)	1250	850	1200
Crushing load (N)	500	800	1000
Water absorption (%)	≥ 10	≤ 5	≤ 3

Table 2 Specification of test beams

Series	Designation	Type of concrete	Dimension (mm) height × width × length	*d* (mm)	*a*/*d*	Longitudinal reinforcement
V-d200	VL2.5–200	L1	250 × 250 × 3300	200	2.5	4 × SD490-D22
	VB2.5–200	B				
	VN2.5–200	N				
	VL3.0–200	L1			3.0	
	VB3.0–200	B				
	VN3.0–200	N				
	VL3.5–200	L1			3.5	
	VB3.5–200	B				
	VN3.5–200	N				
	VL4.0–200	L1			4.0	
	VB4.0–200	B				
	VN4.0–200	N				
	VL5.0–200	L1			5.0	
	VB5.0–200	B				
	VN5.0–200	N				
V-d300	VL4.0–300	L1	375 × 250 × 3700	300	4.0	6 × SD490-D22
	VB4.0–300	B				
	VN4.0–300	N				
V-d500	VL4.0–500	L1	575 × 250 × 5300	500	4.0	6 × SD490-D22
	VB4.0–500	B				
	VN4.0–500	N				
V-d1000	VL3.5–1000	L2	1070× 500 × 10000	1000	3.5	5 × SD490-D35
	VL3.0–1000	L3			3.0	

much. According to the requirement to the density of concrete, therefore, it is important to select the proper type of SLA. It is also possible to use SLA as a part of coarse aggregate in concrete. The shear resisting behaviors of lightweight concrete using blended coarse aggregate with crushed stone and SLA850 is also discussed in this paper.

3. Details of Experimental Test Program

3.1 Test beams

Shear resisting behaviors of SLA concrete were investigated by a series of experimental loading tests on reinforced concrete beams. **Table 2** summarizes the specification of the test beams. The test beams were manufactured according to the following experimental parameters: the type and density of concrete, the effective depth, *d*, and the shear span to effective depth ratio, *a*/*d*.

Three types of concrete, L, B, and N, were used for making the test beam. L is SLA concrete mixed with either SLA850 or SLA1200 as coarse aggregate. L is subdivided into three types: L1 mixed with SLA850 and L2 and L3 mixed with SLA1200. Furthermore, super lightweight fine aggregate was used in L3 by replacing a part of natural sand to adjust the density of the concrete. N is general normal-weight concrete, and B stands for blended aggregate concrete: a part of crushed stone was replaced by SLA. The blended concrete was designed to have almost the same density as the concrete with SLA1200 for a whole of coarse aggregate.

The specified mixes of respective concrete are presented in **Table 3**. L and B were designed to be semi high-fluidity concrete by specifying the slump flow as

Table 3 Specified mix of concrete

Type	Aggregate max. size (mm)	Slump*/ slump flow (mm)	Air content (%)	Water to cement ratio W/C	s/a	Density (kg/m^3)	Unit content (kg/m^3) Water W	Unit content (kg/m^3) Cement C
L1	15	400	5.5	0.45	0.54	1727	170	378
L2	15	450	6.0	0.40	0.52	1826	165	413
L3	15	450	6.0	0.40	0.52	1553	165	413
B	20	400	5.5	0.45	0.54	1836	170	378
N	20	120*	4.5	0.58	0.47	2299	166	289

Type	Unit content (kg/m^3)										
	Powder	Fine aggregate				Coarse aggregate				Chemical admixture	
	LS	SLA	S1	S2	S3	SLA850	SLA1200	G1	G2	SP	WRA
L1	–	–	916	–	–	255	–	–	–	3.97	–
L2	–	–	–	435	440	–	363	–	–	2.48	–
L3	68	154	–	370	–	–	363	–	–	2.48	–
B	–	–	916	–	–	204	–	162	–	3.97	–
N	–	–	–	431	431	–	–	–	982	–	2.89

Table 4 Materials description

Materials		Symbol	Description
Cement	Ordinary Portland cement	C	Density: 3160kg/m^3
Powder	Limestone fine powder	LS	Density: 2700kg/m^3, Blaine: 4260cm^2/g
Fine aggregate	SLA	SLA	Density$^{2)}$: 920kg/m^3, Water absorption (24h): 6.2%
	Sand	S1	Density$^{1)}$: 2580kg/m^3, Water absorption: 1.92%
	Sand	S2	Density$^{1)}$: 2600kg/m^3, Water absorption: 2.54%
	Crushed sand	S3	Density$^{1)}$: 2640kg/m^3, Water absorption: 1.66%
Coarse aggregate	SLA	SLA850	Density$^{2)}$: 850kg/m^3, Water absorption (24h): 3.3%
	SLA	SLA1200	Density$^{2)}$: 1170kg/m^3, Water absorption (24h): 2.8%
	Crushed stone	G1	Density$^{1)}$: 2700kg/m^3
	Crushed stone	G2	Density$^{1)}$: 2660kg/m^3
Chemical admixture	Superplasticizer	SP	
	Water reducing agent	WRA	

1) Measured in saturated surface-dry condition
2) Measured in oven-dry condition

400 to 450mm for verifying their workability during pumping. The basic properties of materials used in the concrete are described in **Table 4**.

The properties of concrete in fresh stage are summarized in **Table 5**, together with the specific cylinder strength at the age of 28 days.

Deformed bars of Grade SD490–D22 and D35 were used as longitudinal reinforcement. The yield strengths of rebars D22 and D35 are 515N/mm^2 and 536N/mm^2, respectively.

The test beam has a rectangular cross section whose breadth is 250mm or 500mm. The geometry and rebar arrangement of beam series V–d200 and V–d300 are shown in **Figure 1**. Those of beam series V–d500 and V–d1000 were designed in the same way as V–d300 and V–d200 respectively; the former has double longitudinal rebars. The effective depth of the test beam is 200, 300, 500, or 1000mm as the experimental parameter and its length varies according to *a/d*. No web reinforcement against shear is provided in the loading span of the test beam to examine the shear capacity with regard to the concrete itself.

On the basis of the experimental parameters described above, each test beam has a unique name as VL2.5–200. "V" represents the beam for shear test. The second symbol indicates the type of concrete. The two numerical values representing *a/d* and the effective depth, *d*, are followed.

In this paper, the shear resisting behaviors of SLA concrete beams were discussed referring to the test result

Table 5 Properties of concrete

Type	Slump flow (mm)	Slump (mm)	Density (kg/m^3)	Air content (%)	Concrete temperature (°C)	f'_c at 28 days (N/mm^2)
L1	380 × 380	–	1711	6.7	12.0	33.7
L2	415 × 390	–	1790	8.7	14.0	47.9
L3	520 × 490	–	1540	6.7	14.5	40.0
B	400 × 380	–	1839	5.1	16.0	31.8
N	–	140	–	3.8	14.5	38.9

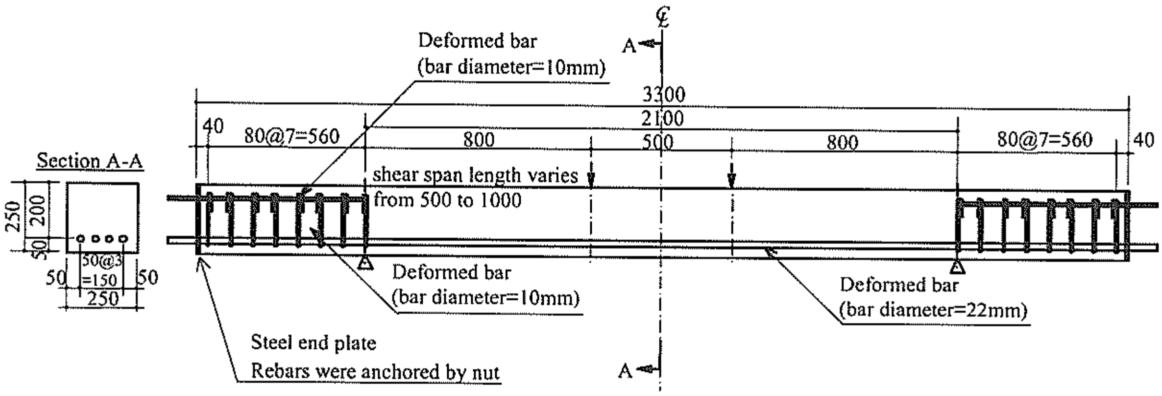

(a) V–d200 (a/d=4.0)

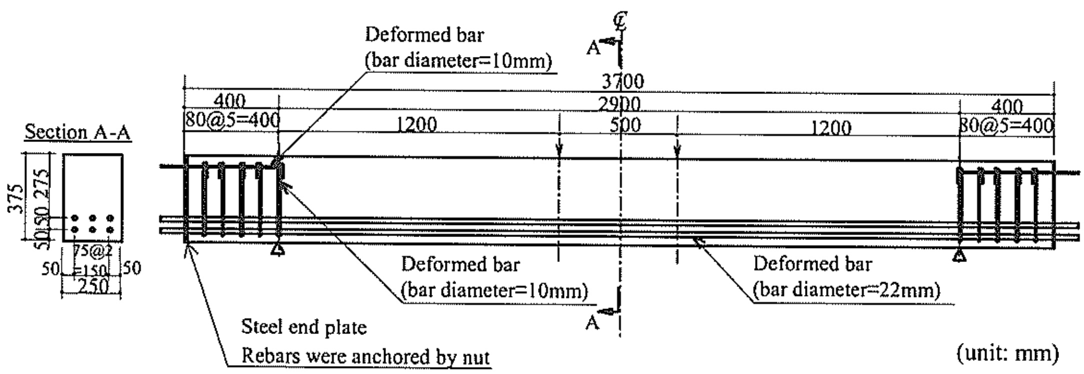

(b) V–d300

Figure 1 Geometry and rebar arrangement of the test beam

on four SLA beams tested in the preliminary study (Yokota et al., 2000b; Funahashi et al., 2001b). The specification of those four beams is presented in **Table 6**. Those beams were designated with the type of concrete, L or N, and the designed density of the concrete: 1200, 1500, 1800, and 2300kg/m^3. The a/d was constant to be 2.94.

3.2 Test procedure

All beams were simply supported and tested in simultaneous shear and flexure using a symmetrical two point loading arrangement that produced a constant moment region at the midspan. The lengths of span and constant moment region were varied to fulfill the experimental parameter of a/d. Teflon sheet was spread in the sliding device at the supports to eliminate friction as much as possible, so that the beam is subjected to little constraint and is possible to move longitudinally. This constraint may affect the mode of shear failure of the beam.

The beams were subjected to monotonically increasing load up to failure by hydraulic jack. During each test, load and deformation characteristics of the test beam were simultaneously measured and crack pattern

Table 6 Specification of beams in the previous test

Designation	Type of concrete	Density of concrete (kg/m^3)	Dimension height × width × length (mm)	d (mm)	a/d	Longitudinal reinforcement
VL−1.8	SLA	1720	400 × 200 × 3400	340	2.94	3 × SD345-D22
VL−1.5	SLA	1620				
VL−1.2	SLA	1310				
VN−2.3	Normal	2260				

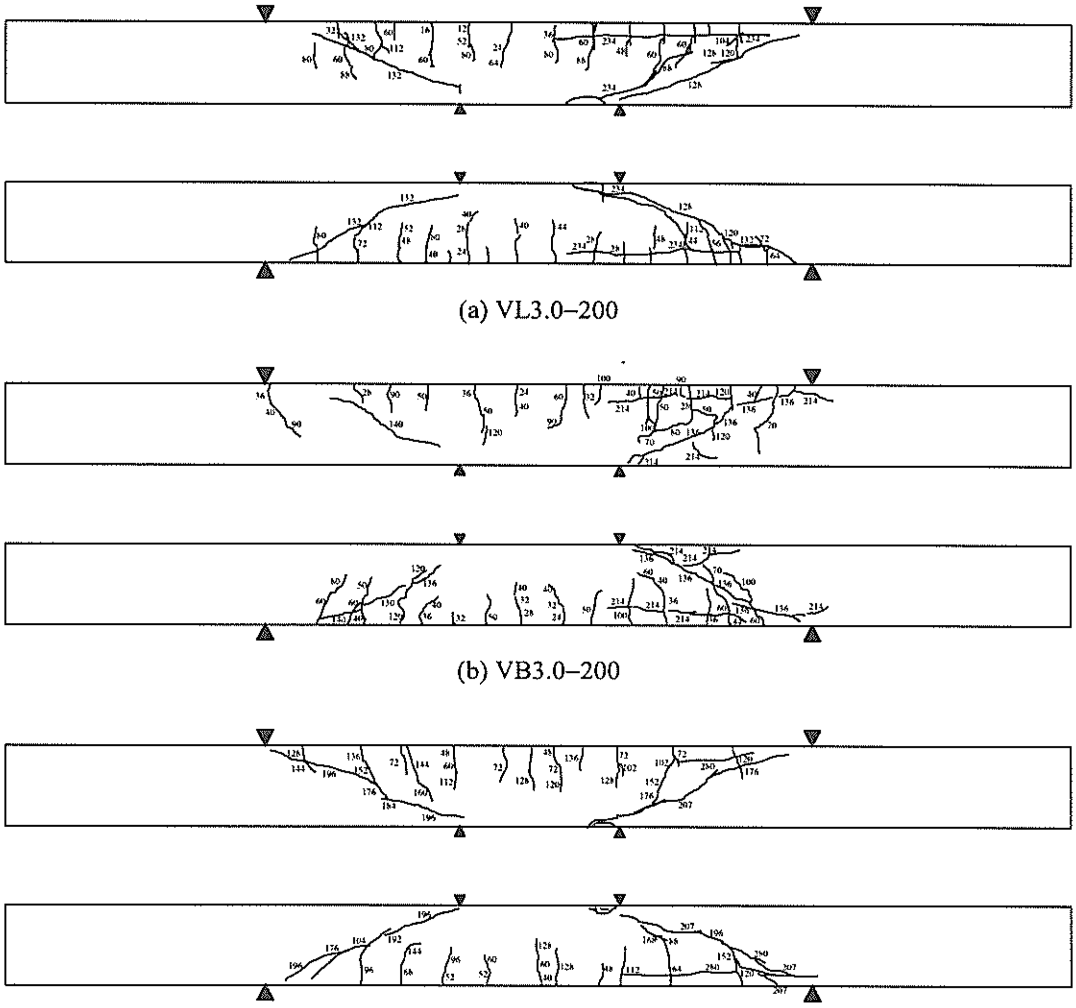

(a) VL3.0−200

(b) VB3.0−200

(c) VN3.0−200

Figure 2 Appearance of cracks (V−d200 series, a/d=3.0)

was traced and recorded. The load applied was measured with a load cell. Deflections of the beam were measured by linear varying displacement transducers at the midspan, at the two loading points, and at the supports. Moreover, strains of rebars were measured by a pair of wire resistant strain gauges in the same sections as those at which deflection was measured. Concrete strain of the compression fiber at the midspan section was also measured by wire resistant strain gauge. Measurement was done by computer controlled data logger at each load step.

At the time of either just before or after the loading test, compressive and tensile strengths of the concrete were investigated by 100mm diameter by 200mm long cylinders and 150mm diameter by 200mm long cylinders, respectively. Those values will be presented in **4.3, Table 7.**

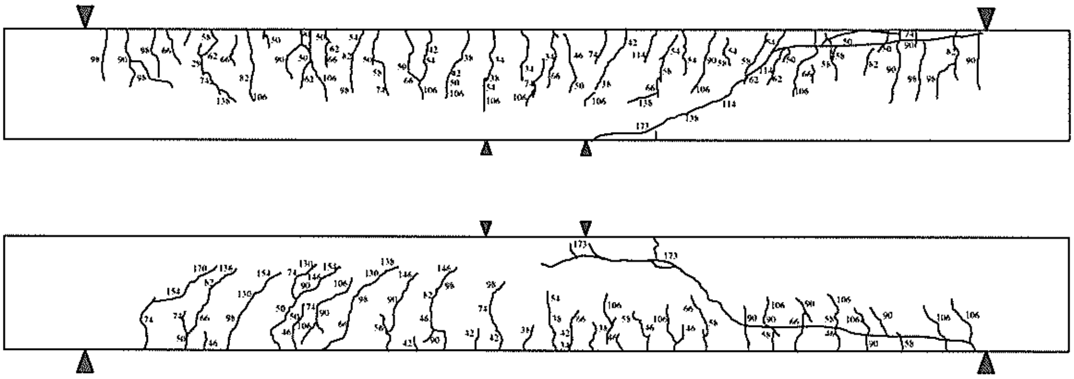

(a) VL4.0–500

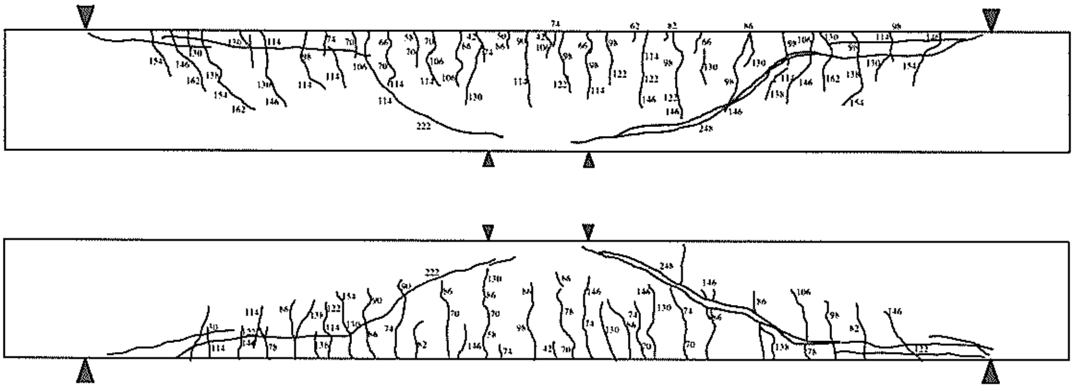

(b) VB4.0–500

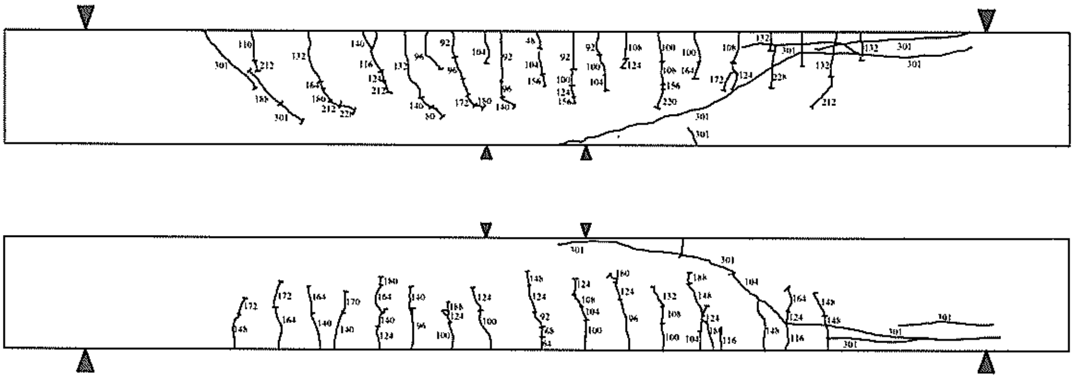

(c) VN4.0–500

Figure 3 Appearance of cracks (V–d500 series)

4. Test Results

4.1 Process of failure

The process of failure of the beam is discussed based on the formation and propagation of cracks.

Figure 2 shows the formation of crack in three beams of V–d200 series up to the maximum load applied. Cracks on the both side surfaces of the beam are drawn in these figures and the numerical values in this figure indicate the load applied in kN at which a target crack propagated.

Several flexural cracks were initiated before a diagonal tension crack occurred. After the formation of a significant diagonal tension crack in each of the two shear spans, the tied-arch mechanism was formed and the failure of the beam was characterized by crushing of concrete in the central region. This mode of failure is

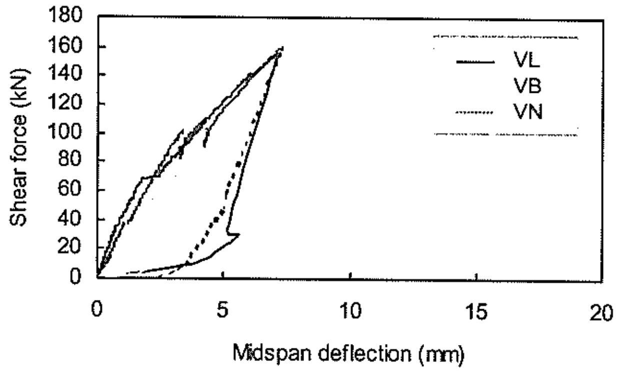

Figure 4 Shear force vs. midspan deflection (V–d200, *a/d*=2.5)

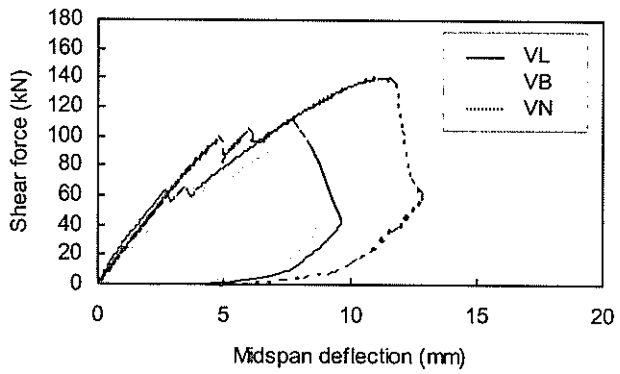

Figure 5 Shear force vs. midspan deflection (V–d200, *a/d*=3.0)

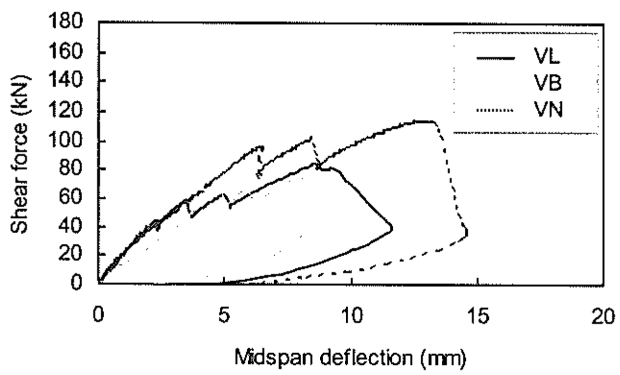

Figure 6 Shear force vs. midspan deflection (V–d200, *a/d*=3.5)

defined as the shear compression failure, SC. In this failure mode, the beams were capable of carrying shear forces even after the significant diagonal tension cracks occurred. That is, the arch resisting mechanism was formed in the beam along the diagonal tension cracks. This transition of failure modes was observed also in all the beams with $a/d \leq 3.5$ of V–d200 series as well as VL3.0–1000.

On the other hand in the remaining beams, the other mode of failure was confirmed; that is, the typical diagonal tension failure, DT. The failure process of DT is shown in **Figure 3** as the crack formation of beams of V–d500 series. V–d500 beams had much more flexural cracks than V–d200 beams shown in **Figure 2** because of the difference of the span and *a/d*. In the mode of DT, immediately after the formation of a diagonal tension crack at the either side of the shear span, the load was sharply dropped and reached to the failure stage. Failure of VL4.0–500 and VN4.0–500 beams as shown in **Figure 3** was exactly categorized in this mode. The beams tested with $a/d \geq 4.0$ as well as VN–2.3 and VL3.5–1000 beams showed this failure except for VB4.0–500 beam.

VB4.0–500 beam showed the slightly different failure mode. That is, even after a diagonal tension crack occurred, the load did not drop and became large up to formation of another diagonal tension crack at the other shear span. The final stage was characterized by crushing of the top part of concrete at the tip of the diagonal crack. VL–1.2, VL–1.5, and VL–1.8 beams showed the same failure mode.

The above two failure modes are both diagonal tension failure. In this paper, however, the two modes will be distinguished each other: the former is DT1 and the latter is DT2.

The difference of the failure mode was brought about primarily by the parameter of *a/d*, neither by the type of concrete nor by the effective depth. When the density of concrete became smaller, the failure mode of SLA beams changed into DT2 failure mode as observed in VL–1.5 and VL–1.2 beams.

4.2 Load displacement relationship

The process of shear failure described in **4.1** will be discussed by the relationship between the shear force and displacement. **Figures 4** to **8** show the shear force versus midspan deflection curves of V–d200 beams. The shear force is defined as a half of the load applied. The curves of beams that showed SC failure mode had three bending points as shown in **Figures 4** to **6**. The first bending point indicates the formation of the first diagonal tension crack and the second one does the formation of the diagonal tension crack in another shear span. The last one is coincident with the failure of the beam and after this point the shear force rapidly decreased. Therefore, the shear force at this point is defined as the ultimate shear capacity.

The beams failed by DT1 failure mode showed the different relationship as those failed by SC as presented **Figures 7** and **8**. Some of the beams had two bending points there, but the first one corresponded to the

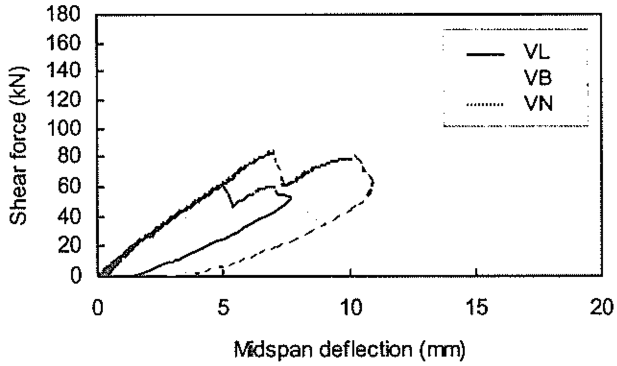

Figure 7 Shear force vs. midspan deflection (V–d200, a/d=4.0)

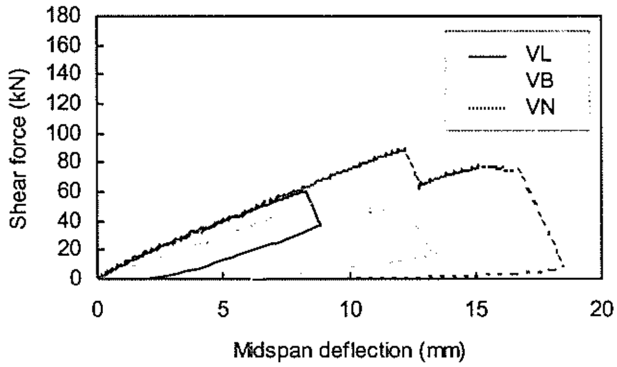

Figure 8 Shear force vs. midspan deflection (V–d200, a/d=5.0)

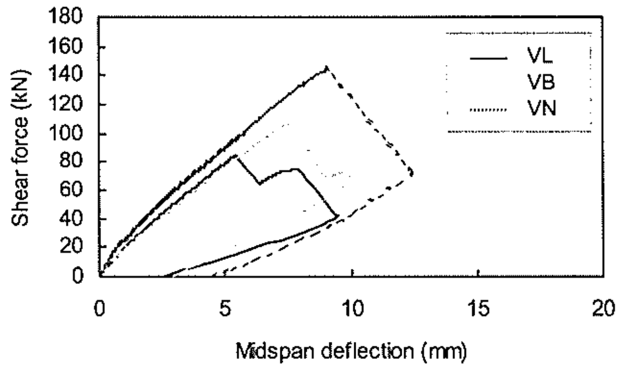

Figure 9 Shear force vs. midspan deflection (V–d300, a/d=4.0)

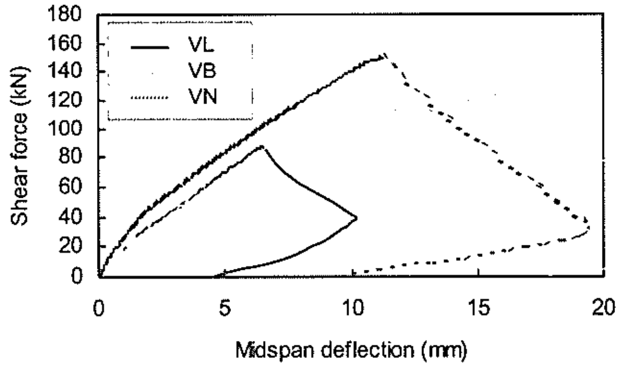

Figure 10 Shear force vs. midspan deflection (V–d500, a/d=4.0)

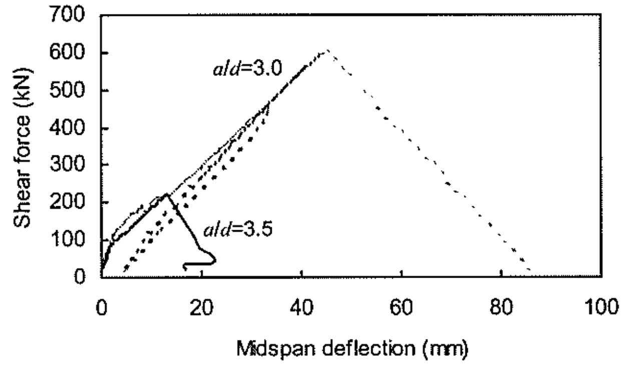

Figure 11 Shear force vs. midspan deflection (V–d1000)

maximum shear force. When the effective depth became large, as shown in **Figures 9** and **10**, this trend was rather distinct; the beams that failed by DT1 mode were brittle.

The load-displacement relationship of VB4.0–500 beam was similar to that of the beams with SC failure mode. The difference of the failure modes between SC and DT2 is not clearly distinctive from the viewpoint of load-displacement characteristics. Those characteristics of the remaining beams are shown in **Figure 11**, which are the same as the beams described before.

There was no significant difference in the rigidity of the beam regardless of small Young's modulus in SLA concrete.

4.3 Shear carrying capacity

On the basis of the experimental test results of crack formation and the relationship between the shear force and displacement, the failure mode, the diagonal tension cracking load (shear force), and the shear capacity are summarized in **Table 7**. The density of concrete and strengths of concrete at the test are also presented in the table. The diagonal tension cracking load is defined as the shear force when the first diagonal tension crack was formed.

The shear capacities of the beams mixed with SLA at the initiation of a diagonal tension crack were almost the same as compared between VL and VB beams, while

Table 7 Summary of the experimental test results

Designation	Density of concrete (kg/m³)	f'_c (N/mm²)	f_t (N/mm²)	Failure mode	Shear capacity at diagonal cracking stage		Ultimate shear capacity		$V_{u,exp}$ / $V_{c,exp}$
					$\tau_{c,exp}$ (N/mm²)	$V_{c,exp}$ (kN)	$\tau_{u,exp}$ (N/mm²)	$V_{u,exp}$ (kN)	
VL2.5–200	1770	31.2	1.72	SC	1.36	68.0	3.07	153.5	2.26
VB2.5–200	1850	33.4	2.45	SC	1.39	69.5	2.25	112.5	1.62
VN2.5–200	2333	33.3	2.98	SC	2.04	102.0	3.20	160.0	1.57
VL3.0–200	1770	31.2	1.72	SC	1.28	64.0	2.24	112.0	1.75
VB3.0–200	1850	33.4	2.45	SC	1.36	68.0	2.14	107.0	1.57
VN3.0–200	2333	33.3	2.98	SC	1.96	98.0	2.80	140.0	1.43
VL3.5–200	1770	31.2	1.72	SC	1.18	59.0	1.69	84.5	1.43
VB3.5–200	1850	33.4	2.45	SC	1.31	65.5	1.51	75.5	1.15
VN3.5–200	2333	33.3	2.98	SC	1.94	97.0	2.30	115.0	1.19
VL4.0–200	1770	31.2	1.72	DT1	1.23	61.5	1.23	61.5	1.0
VB4.0–200	1850	33.4	2.45	DT1	1.33	66.5	1.33	66.5	1.0
VN4.0–200	2333	33.3	2.98	DT1	1.67	83.5	1.67	83.5	1.0
VL5.0–200	1770	31.2	1.72	DT1	1.21	60.5	1.21	60.5	1.0
VB5.0–200	1850	33.4	2.45	DT1	1.34	67.0	1.34	67.0	1.0
VN5.0–200	2333	33.3	2.98	DT1	1.77	88.5	1.77	88.5	1.0
VL4.0–300	1770	29.1	1.63	DT1	1.13	85.0	1.13	85.0	1.0
VB4.0–300	1816	34.8	1.96	DT1	1.41	106.0	1.41	106.0	1.0
VN4.0–300	2333	37.6	2.58	DT1	1.93	144.5	1.93	144.5	1.0
VL4.0–500	1793	31.2	1.69	DT1	0.69	86.5	0.69	86.5	1.0
VB4.0–500	1832	34.5	2.57	DT2	0.89	111.0	0.99	124.0	1.12
VN4.0–500	2340	41.2	3.05	DT1	1.20	150.5	1.20	150.5	1.0
VL3.5–1000	1810	37.7	2.51	DT1	0.44	222.2	0.44	222.2	1.0
VL3.0–1000	1560	34.1	2.21	SC	0.35	177.2	1.20	598.8	3.38
VL–1.8	1720	33.7	2.87	DT2	0.63	43.0	1.30	88.2	2.05
VL–1.5	1620	45.0	2.01	DT2	0.61	41.8	0.90	61.4	1.47
VL–1.2	1310	33.3	1.70	DT2	0.54	36.9	0.87	59.2	1.61
VN–2.3	2260	23.0	2.17	DT1	1.17	79.8	1.17	79.8	1.0

Note) f'_c : compressive strength of concrete, f_t : tensile strength of concrete, V : shear force, τ : shear stress

those of the beams of general normal-weight concrete, VN, were considerably higher than VL and VB beams. Even if normal crushed stone was used with SLA, the effect of the particle geometry of SLA was considered not to be ignorable.

Comparing the ultimate shear capacities of the beams that showed SC failure mode, the effect of SLA was rather significant. The ratios of ultimate shear capacity to diagonal cracking shear capacity of VL beams were approximately 1.4 to 2.3; the higher ratio was obtained as *a*/*d* became smaller. Those of VB and VN beams were about 1.3 to 1.6 and 1.2 to 1.5 respectively. When SLA is used in a concrete beam with smaller *a*/*d*, the diagonal cracking load will be smaller, but the beam can carry further shear forces after the cracking.

Regardless of the mode of failure, VN beams carried larger shear force compared to other beams with

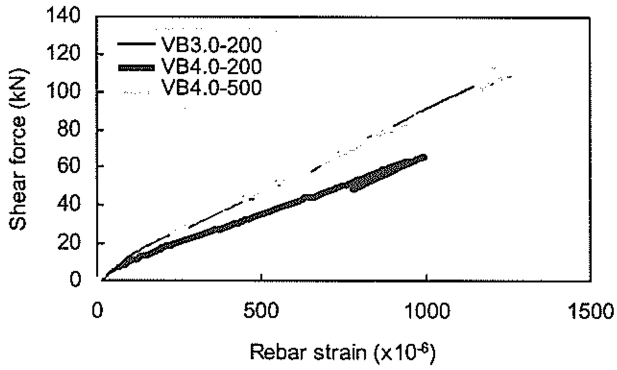

Figure 12 Relationship between shear force and longitudinal rebar strain at the midspan

Table 8 Summary of the calculation results and comparison to experimental results

Designation	Calculated shear capacity (kN)				Comparison to the experimental results					
	(a)	(b)	(c)	(d)	Diagonal cracking			Ultimate		
	η_s Eq.(2) $\eta_s = 0.7$	η_s Eq.(3) $\eta_s = 0.7$	η_s Eq.(3) η_s=Eq(5)	Eq.(6)	vs.(a)	vs.(b)	vs.(c)	vs.(a)	vs.(b)	vs.(d)
VL2.5–200	48.0	62.9	60.7	122.5	1.42	1.08	1.12	–	–	1.25
VB2.5–200	49.1	64.4	66.3	128.4	1.41	1.08	1.05	–	–	0.88
VN2.5–200	70.1	91.8	91.8	128.0	1.46	1.11	1.11	–	–	1.25
VL3.0–200	48.0	58.4	56.3	88.8	1.33	1.10	1.14	–	–	1.26
VB3.0–200	49.1	59.8	61.6	93.1	1.38	1.14	1.10	–	–	1.15
VN3.0–200	70.1	85.3	85.3	92.8	1.40	1.15	1.15	–	–	1.51
VL3.5–200	48.0	55.2	53.2	67.0	1.23	1.07	1.11	–	–	1.26
VB3.5–200	49.1	56.5	58.2	70.2	1.33	1.16	1.12	–	–	1.07
VN3.5–200	70.1	80.6	80.6	70.0	1.38	1.20	1.20	–	–	1.64
VL4.0–200	48.0	52.8	50.9	52.3	1.28	1.16	1.21	1.28	1.16	–
VB4.0–200	49.1	54.0	55.7	54.7	1.35	1.23	1.19	1.35	1.23	–
VN4.0–200	70.1	77.1	77.1	54.6	1.19	1.08	1.08	1.19	1.08	–
VL5.0–200	48.0	49.4	47.7	34.2	1.26	1.22	1.27	1.26	1.22	–
VB5.0–200	49.1	50.6	52.2	35.8	1.36	1.32	1.28	1.36	1.32	–
VN5.0–200	70.1	72.2	72.2	35.7	1.26	1.23	1.23	1.26	1.23	–
VL4.0–300	63.6	70.0	67.5	59.3	1.34	1.21	1.26	1.34	1.21	–
VB4.0–300	67.5	74.3	74.4	66.8	1.57	1.43	1.42	1.57	1.43	–
VN4.0–300	99.0	108.9	108.9	70.4	1.46	1.33	1.33	1.46	1.33	–
VL4.0–500	80.5	88.6	87.1	70.0	1.07	0.98	0.99	1.07	0.98	–
VB4.0–500	83.3	91.6	93.0	74.9	1.33	1.21	1.19	1.49	1.35	–
VN4.0–500	126.2	138.9	138.9	84.3	1.19	1.08	1.08	1.19	1.08	–
VL3.5–1000	231.2	265.9	265.2	340.9	0.96	0.84	0.84	0.96	0.84	–
VL3.0–1000	223.7	272.2	217.2	380.7	0.79	0.65	0.82	–	–	1.57
VL–1.8	48.1	59.0	54.5	82.0	0.89	0.73	0.79	1.83	1.49	–
VL–1.5	53.0	65.0	54.9	99.3	0.79	0.64	0.76	1.16	0.94	–
VL–1.2	48.0	58.8	36.1	81.3	0.77	0.63	1.02	1.23	1.01	–
VN–2.3	60.5	74.2	72.2	63.4	1.32	1.08	1.10	1.32	1.08	–

the same experimental parameters. Moreover, the shear capacity of the beam became small as the density of concrete was decreased. The characteristics of such reduction will be discussed in **5.1**. Use of crushed stone mixed with SLA as coarse aggregate in the concrete provided slight increase in shear capacity in case of DT1 failure mode.

The strains of longitudinal rebar at the midspan section of the beam are shown in **Figure 12** for ensuring the mode of failure. In this figure, beams of three types of failure modes are selected: VB3.0–200 with SC, VB4.0–200 with DT1, and VB4.0–500 with DT2. In particular, un-yield of a longitudinal rebar has to be confirmed in DT failure mode. All the beams presented in this figure had almost the same strain characteristics and no longitudinal rebars yielded up to failure of the beam.

5. Shear Resisting Behaviors

5.1 Effect of the density of concrete

It was made clear from the experimental results that the shear resisting capacity of SLA beams is dependent on the density of concrete. The effect of the density of concrete to shear resisting capacity is not taken into account in the current design calculation in Japan as mentioned before. However, in the draft of revised version of Eurocode-2 (Walraven, 2000), a density of concrete is considered as the conversion term that is a factor to calculate the shear capacity of lightweight concrete beams using that of general normal-weight concrete beams. The conversion term, η_s, is expressed as follows:

$$\eta_s = 0.4+0.6\,(\rho/2400) \qquad (1)$$

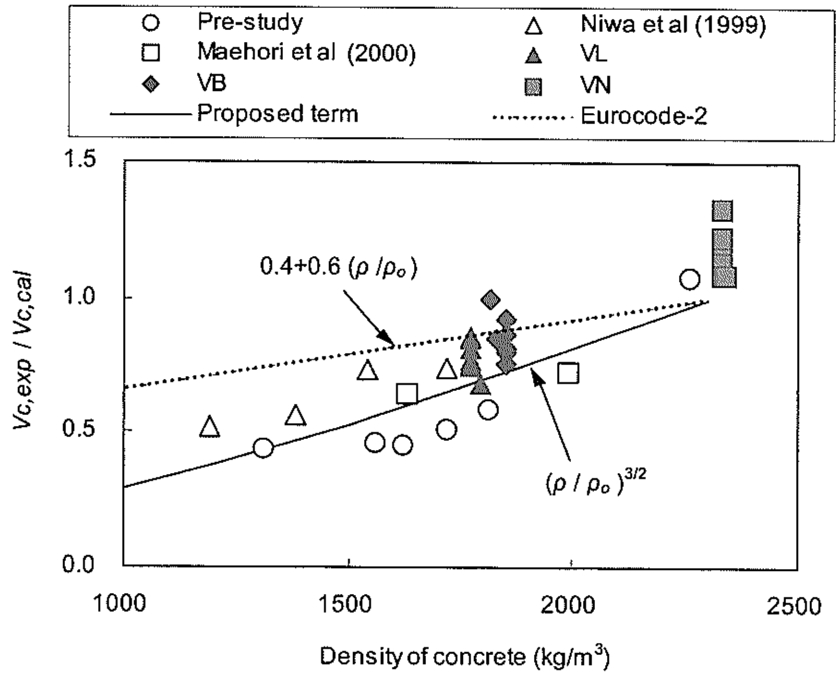

Figure 13 Shear capacity relating diagonal tension crack versus density of concrete

where, ρ is a density of concrete in kg/m^3. This term originally derives from that regarding the tensile strength of concrete. The density of normal concrete, ρ_o, is specified to be 2300 kg/m^3 in Japan; therefore 2400 in Eq. (1) will be replaced by 2300.

In the JSCE design standard for concrete structures (1996), the shear carrying capacity of a reinforced concrete beam without web reinforcement such as stirrups is calculated as follows:

$$V_{c.cal} = 0.20\sqrt[3]{f'_c}\sqrt[3]{100p_w}\sqrt[4]{1000/d}\ b_w d \quad (2)$$

where, f'_c is the compressive strength of concrete (N/mm^2), p_w is the longitudinal reinforcement ratio, d is the effective depth of a beam (mm), and b_w is the width of a beam. In the original equation, the effects of prestressing and axial forces are taken into account, but they are omitted in Eq. (2) because of no relation to this study.

Eq. (2) is a simplified equation based on the empirical study conducted by one of the authors (Niwa et al., 1987). The original equation explicitly considers the effect of a/d as follows:

$$V_{c.cal} = 0.20\sqrt[3]{f'_c}\sqrt[3]{100p_w}\sqrt[4]{1000/d}\left(0.75+\frac{1.4}{a/d}\right)b_w d \quad (3)$$

As easily understood, the JSCE equation is equivalent to the case of a/d=5.6. Since the value of a/d is one of the important experimental parameters in this study, Eq. (3) is also used for discussion.

For calculating the shear capacity of SLA beams with the current design equations as Eqs. (2) and (3), the constant value of 0.7 is specified as the conversion term; that is, η_s=0.7. The calculated values of the tested beams with the constant η_s are presented in **Table 8**, columns **(a)** and **(b)**. Most of the beams when the density of concrete is larger than about 1700kg/m^3 were estimated to be on the safe side: the ratios of experimental results to calculated ones were approximately 1.3 to 1.4 by Eq. (2) and 1.1 to 1.3 by Eq. (3). For the tested beams whose density is smaller than about 1700kg/m^3, the calculated values were rather small compared to the experimental results.

Figure 13 shows the shear load carrying capacity at diagonal tension cracking of SLA beams against the density of concrete. The test results with SLA concrete beams done by Niwa et al. (1999) and Maehori et al. (2000) are also plotted in this figure. In case of using η_s=0.7, the density of 1700 to 1800kg/m^3 is the lower limit value that this η_s is applicable. The conversion term in the Eurocode-2 calculated larger capacity than the experimental results when using Eq.(3) for estimating shear capacity. Therefore, the new conversion term will be proposed here.

The shear strength of concrete to govern the shear capacity of concrete beams has not well been quantified. If the shear failure mechanism is considered to have close relation to the tensile splitting strength of concrete, a conversion term for calculating the tensile strength of lightweight concrete is worth taking into account. The

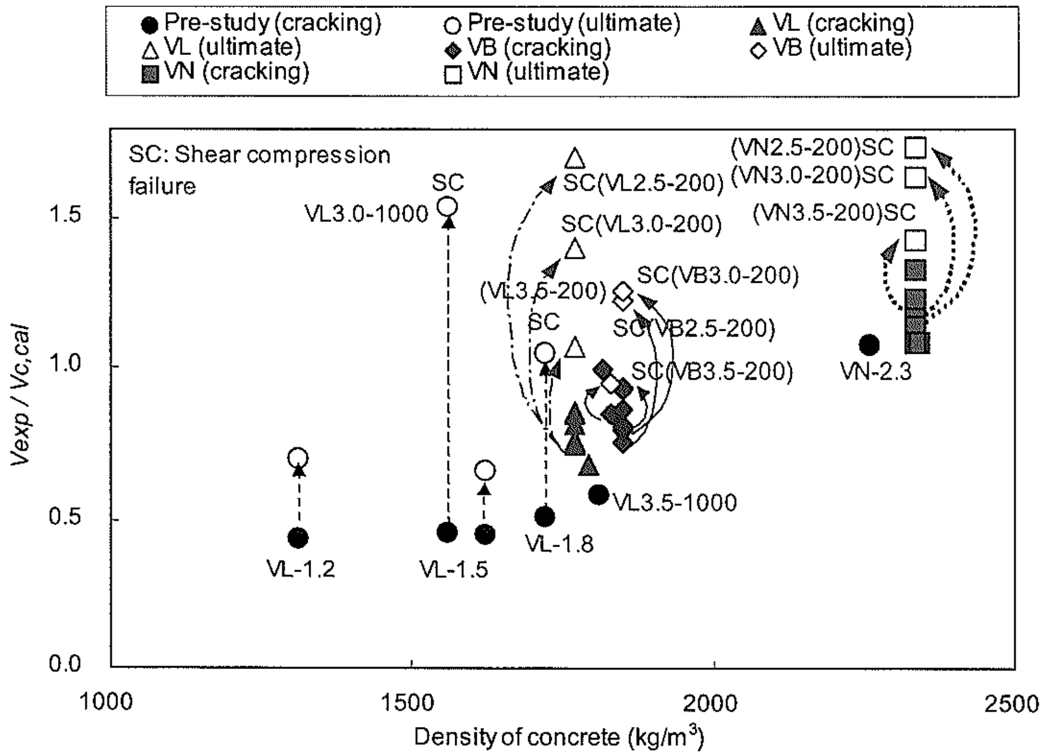

Figure 15 $V_{exp} / V_{c,cal}$ versus density of concrete

conversion term for tensile strength of concrete is shown in **Figure 14**. For calculating the tensile strength of concrete, f_t, from its compressive strength, the following equation is currently applied:

$$f_t = 0.27 f'^{2/3}_c \quad (4)$$

In this figure, the ratio of the experimental value of the tensile strength to the calculated value by Eq. (4) is plotted against the density of concrete. From the authors' previous study (Funahashi et al., 2001b), the conversion terms relating to basic mechanical properties of SLA concrete can be expressed as $\eta_t = (\rho / \rho_o)^n$, where n is a certain number. Applying this format of the function to calculate the tensile strength, it is most fitted to set n=1/2 for SLA concrete. The predicted line of using n=1/2 is shown in **Figure 14**. The calculated strengths with n=1/2 are slightly smaller than the average of experimental ones, but the applicability is confirmed. There is very little difference by comparing to η_s of Eq. (1). Therefore, the conversion term to calculate the shear capacity of SLA beams will be expressed as the similar way to η_t.

Through try-and-error examination to find the most reasonable one, the conversion term, η_s to predict the shear capacity of SLA beams is proposed as follows:

$$\eta_s = (\rho / \rho_o)^{3/2} \quad (5)$$

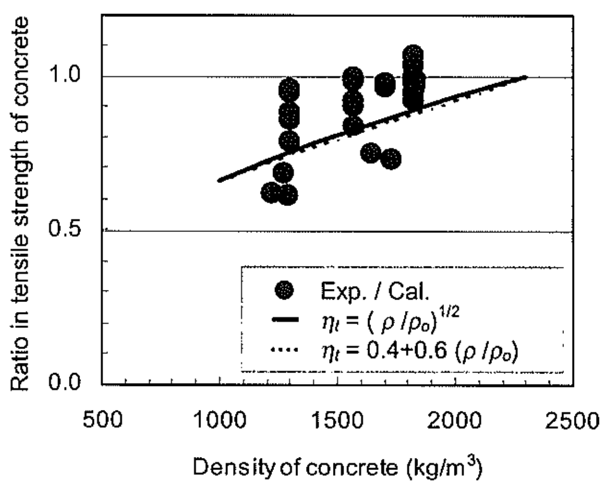

Figure 14 Prediction of tensile strength by the density of concrete

The accuracy of this proposed conversion term is confirmed in **Figure 13** and **Table 8** at the shaded columns. This conversion term is not the best fit one to explain the experimental results. However, considering the following reasons, Eq. (5) is concluded to be applicable: 1) the equation is rather simple and 2) the equation is consistent with the other basic mechanical

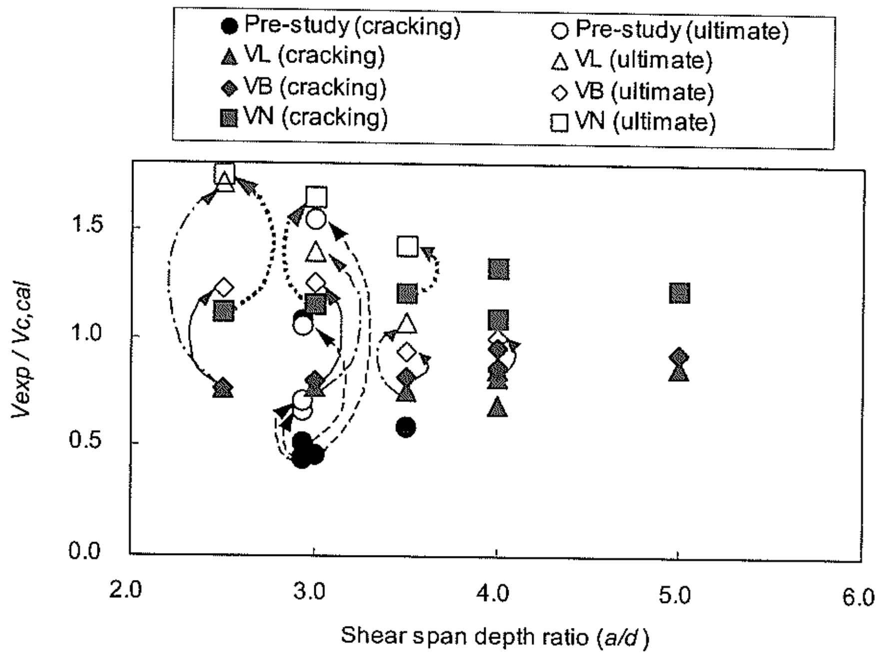

Figure 16 V_{exp} / $V_{c,cal}$ versus shear span to depth ratio

properties of SLA concrete such as tensile strength and Young's modulus.

For calculating the shear capacity in case of SC failure mode, the shear compression capacity, $V_{u,cal}$, should be evaluated. The equation to calculate this is given by the following equation:

$$V_{u,cal} = \frac{0.244 f_c'^{2/3} \left(1+\sqrt{100 p_w}\right)\left(1+3.33 r/d\right)}{1+(a/d)^2} b_w d \qquad (6)$$

where, r is the width of load applied. Except for VB2.5–200, all the beams showed higher shear capacity than the calculated one as presented in **Table 8**. Since shear compression failure will be governed by the compressive strength of concrete, the conversion term is not required for calculation.

Figure 15 shows the relationship between the shear capacity of tested beams at either diagonal tension failure or shear compression failure and the density of concrete. The shear force at diagonal tension cracking of SLA beams was approximately 45 to 75% as small as that at failure. Shibata et al. (1998) studied the fracture mechanics of SLA concrete and showed that SLA concrete had considerably lower ability to absorb energy along the face of a crack than general normal-weight concrete. This characteristic might cause the lower shear capacity at diagonal tension cracking in SLA concrete beams. As the density of concrete became smaller, this difference was more significant. On the other hand, in case of SLA concrete with a density of about 1800kg/m^3, the difference between those forces was small. Therefore, it is concluded that the shear capacity depending on the failure mode was greatly affected not only by the density of concrete but also by the shear span to effective depth ratio, a/d, which will be described later.

5.2 Effect of shear span to effective depth ratio

Figure 16 shows the relationship between the shear capacity of tested beams with either DT or SC failure modes and a/d. When a/d was equal to be 5.0, all the beams failed by DT failure mode. As a/d became smaller, the shear force of SC failure mode was larger than that of DT failure mode. Moreover, comparing of SLA concrete beams to normal-weight concrete beams, the transitional a/d between the two failure modes of SLA concrete beams had a tendency to become larger. This may be derived from low shear capacity of SLA concrete beams.

This difference is schematically shown in **Figure 17**. The shear capacity of a normal-weight reinforced concrete beam is governed by both the diagonal tension cracking (DT) force and the shear compression failure (SC) force with the arch mechanism. A broken line and a dash-dotted line in this figure are shear capacity regarding DT and SC respectively. The transitional value of a/d is generally 2.0 to 2.5 in normal-weight concrete. On the other hand, an SLA concrete beam showed lower diagonal crack load. Therefore, the transitional value of a/d will shift to be large on the assumption that the arch

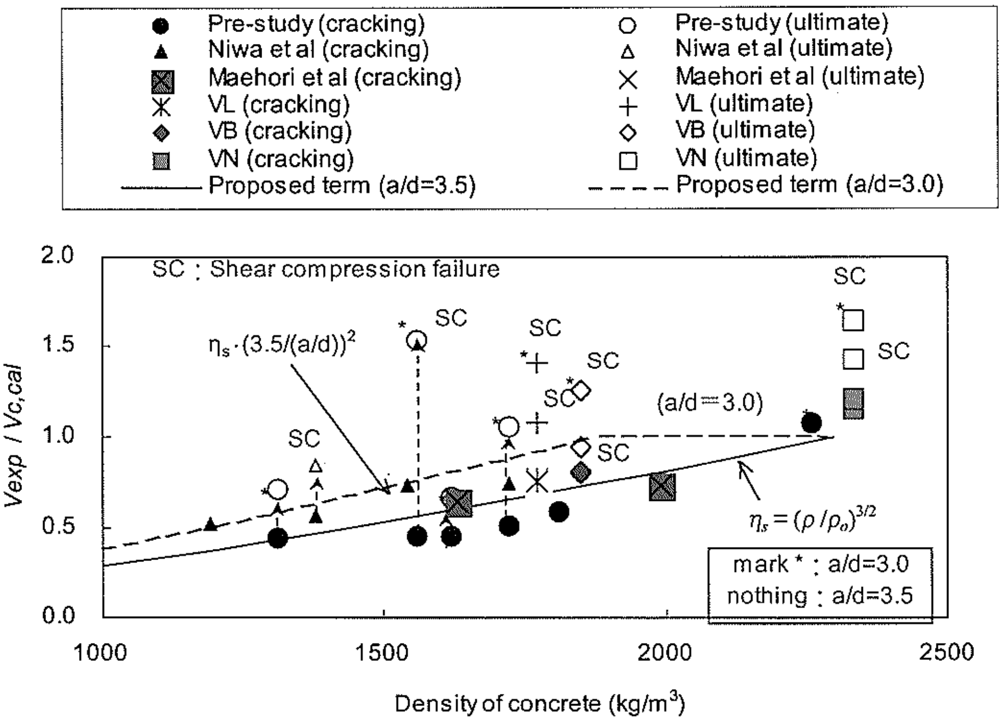

Figure 18 Shear capacity of SLA beam with DT and SC failure modes

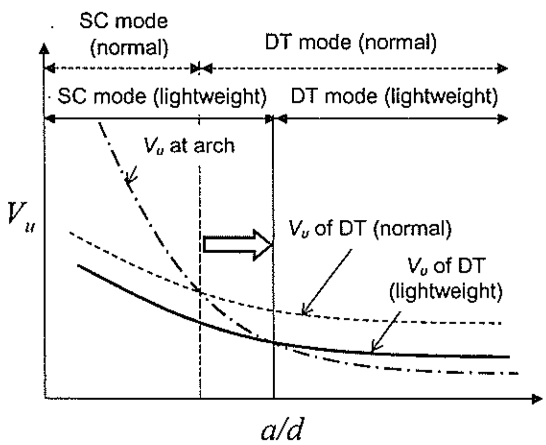

Figure 17 The mode of failure against *a/d*

load is not significantly differed because this type of failure is dominated by compressive strength of concrete.

Figure 18 shows the shear capacity of tested beams and at diagonal tension cracking and at ultimate normalized by calculated shear capacity with Eq. (3). The solid line represents the predicted result using the proposed η_s. The results by Niwa et al. (1999) and Maehori et al. (2000) are also plotted there. As indicated in the previous section, the beams with a/d=3.0, marked with "*", experienced DT failure at first and consequent SC failure at the ultimate except for normal-weight concrete beams. In case of a/d=3.5, however, most of the beams showed DT failure mode.

A SLA beam with a/d=3.5 that is likely to fail with DT failure mode is possible to be predicted its shear capacity by using the proposed conversion term in this paper, η_s. On the other hand, a beam with a/d=3.0 is required to consider the tied-arch resisting mechanism after diagonal tension cracking, but this does not always happen. Within the transitional region from DT failure to SC failure, the increment in shear capacity is considered as a function of a/d. The dashed line in **Figure 18** is one example to take into account such mechanism: another conversion term as $\eta_s(3.5/(a/d))^2$; but not been well examined in this study.

6. Conclusions

The following conclusions were drawn from the experimental shear loading tests on various SLA concrete beams:

(1) The shear capacity of SLA concrete beams at diagonal tension cracking decreased as the density of concrete became small. The conversion term was proposed to express this reduction with the density of concrete, ρ, as $(\rho/\rho_o)^{3/2}$.

(2) SLA concrete beams likely to transfer its failure mode from the diagonal splitting failure to shear compression failure at the larger shear span to effective depth ratio compared to that of general normal-weight concrete.

(3) Regarding the change in shear failure mode, the transitional value of the shear span to effective depth ratio was 3.0-3.5 in SLA concrete beams.

(Received on May 30, 2001)

Acknowledgements

The presented experimental test has been carried out as a part of a collaborative research program on "the application of SLA concrete to marine concrete structures" undertaken by Maeda Corporation, Taiheiyo Cement Co. Ltd, Tokyo Institute of Technology and Port and Harbour Research Institute. The authors would like to extend their appreciation to Dr. T. Okamoto, Taiheiyo Cement and Dr. K. Yokozawa, Maeda Corporation for their instructive suggestion and useful discussion. Messrs. T. Tochigi and S. Ishida, Taiheiyo Cement, are fully acknowledged for their cooperation in making SLA concrete. The authors would like to gratitude Mr. K. Abe, Niigata Investigation and Design Office, Ministry of Land, Infrastructure and Transport for his support.

References

Funahashi, M., Hara, N., Yokota, H., and Niwa, J. (2001a): Shear Capacity of RC Beams of Super Lightweight Aggregate Concrete, Proc. of the Japan Concrete Institute, Vol.23, No.3, pp.919-924. *(in Japanese)*

Funahashi, M., Hara, N., Yokota, H., Yamaji, T., Okamoto, T., and Niwa, J. (2001b): Mechanical Properties of Super Lightweight Aggregate Concrete, *Proc. of the 3rd International Conference on Concrete Under Severe Conditions*, Vancouver, pp.1336-1343.

Japan Society of Civil Engineers (1996): *Standard Specification for Design and Construction of Concrete Structures*.

Maehori, S., Tamura, T., Okamoto, T., and Niwa, J. (2000): Shear Resistance of Large Scale Prestressed Concrete Beams Using Super Lightweight Aggregates, *Proceedings of the Third Regional Symposium on Infrastructure Development in Civil Engineering*, Tokyo, pp.635-642.

Niwa, J., Hamada, Y., Tamura, S., and Okamoto, T. (1999): Shear Resistance of Prestressed Concrete Beams Using High Performance Lightweight Aggregates, *The 7th East Asia-Pacific Conference on Structural Engineering and Construction*, Kochi, pp.1051-1056.

Niwa, J., Yamada, K., Yokozawa, K., and Okamura, H. (1987): Revaluation of the Equation for Shear Strength of Reinforced Concrete Beams without Web Reinforcement, *Concrete Library International of Japan Society of Civil Engineers*, No.9, pp.65-85.

Okamoto, T., Ishikawa, Y., Tochigi, T., and Sasajima, M. (1999): High Performance Lightweight Concrete, *Concrete Journal*, Vol.37, No.4, pp.12-18. *(in Japanese)*

Shibata, T., Okamoto, T., Hayano, H., and Ishikawa, Y. (1998): A Study on Fractural Behavior of Concrete Used by High-Performance Lightweight Aggregates, *Proc. of the Japan Concrete Institute*, Vol.20, No.2, pp.49-54. *(in Japanese)*

Walraven, J. (2000): Design of structures with lightweight concrete: Present status of revision of EC–2, *Proc. of the Second International Symposium on Structural Lightweight Aggregate Concrete*, Kristiansand, pp.57-70.

Yokota, H., et al. (2000a): Super-Lightweight Concrete Caisson for Port Structures, *IABSE 16th Congress, Structural Engineering for Meeting Urban Transportation Challenges*, Lucerne, pp.246-247.

Yokota, H., et al. (2000b): Fundamental Study on the Application of Super-Lightweight Concrete to Port Structures, *Technical Note of PHRI*, No.967, pp.1-31. *(in Japanese)*

List of Symbols

$V_{c,cal}$: calculated shear capacity at diagonal cracking
$V_{u,cal}$: calculated shear capacity at ultimate
a : shear span of a beam
b_w : width of a beam
d : effective depth of a beam
f'_c : compressive strength of concrete
f_t : tensile strength of concrete
p_w : longitudinal reinforcement ratio
η : conversion term in general
η_t : conversion term for tensile strength
η_s : conversion term for shear capacity
ρ : density of concrete
ρ_o : density of general normal-weight concrete ($=2300 kg/m^3$ in this paper)
τ : shear stress